Impact of particulate organic matter on the relative humidity dependence of light scattering: A simplified parameterization

P. K. Quinn,[1] T. S. Bates,[1] T. Baynard,[2] A. D. Clarke,[3] T. B. Onasch,[4] W. Wang,[5] M. J. Rood,[5] E. Andrews,[6] J. Allan,[7] C. M. Carrico,[8] D. Coffman,[1] and D. Worsnop[4]

Received 5 August 2005; revised 19 September 2005; accepted 24 October 2005; published 30 November 2005.

[1] Measurements during recent field campaigns downwind of the Indian subcontinent, Asia, and the northeastern United States reveal a substantial decrease in the relative humidity dependence of light scattering, $f_{\sigma sp}(RH)$, with increasing mass fraction of particulate organic matter (POM) for submicrometer aerosol. Using data from INDOEX (INDian Ocean EXperiment), ACE Asia (Aerosol Characterization Experiment – Asia), and ICARTT (International Consortium for Atmospheric Research on Transport and Transformation), we have identified, within measurement limitations, the impact of POM on the $f_{\sigma sp}(RH)$ of accumulation mode sulfate-POM mixtures. The result is a parameterization that quantifies the POM mass fraction - $f_{\sigma sp}(RH)$ relationship for use in radiative transfer and air quality models either as input or as validation. The parameterization is valid where the aerosol consists of an internally mixed sulfate-carbonaceous accumulation mode and other externally mixed components (e.g. sea salt, dust) and is applicable on both global and regional scales. **Citation:** Quinn, P. K., et al. (2005), Impact of particulate organic matter on the relative humidity dependence of light scattering: A simplified parameterization, *Geophys. Res. Lett.*, *32*, L22809, doi:10.1029/2005GL024322.

1. Introduction

[2] Direct climate forcing (DCF) by anthropogenic aerosol results from changes in top-of-atmosphere and surface net fluxes due to absorption and scattering of solar radiation. The absorption and scattering of solar radiation by anthropogenic aerosols also affects air quality as it impairs visibility. The magnitude of DCF and visibility impairment is affected by changes in particle light scattering due to water uptake under conditions of increasing relative humidity (RH). Chemical transport models (CTMs) generate concentration fields of individual aerosol chemical components (sulfate, particulate organic matter (POM), elemental carbon (EC), dust, and sea salt) which are then used as input to radiative transfer models (RTMs) for the calculation of DCF and air quality models for forecasting visibility. Currently, these calculations are performed with a variety of simplifying assumptions concerning the RH dependence of light scattering by the aerosol. Chemical components often are treated as externally mixed with a unique $f_{\sigma sp}(RH)$ assigned to each component. In this context, sulfate and POM are treated independently such that $f_{\sigma sp}(RH)$ for sulfate is based on theoretical calculations or laboratory measurements while POM is assumed to be hydrophobic or to have $f_{\sigma sp}(RH)$ scalable to or equal to that of sulfate [e.g., *Haywood et al.*, 1999; *Chin et al.*, 2002]. However, both laboratory and field measurements indicate that POM that is internally mixed with water soluble salts can reduce the particles' hygroscopic response, which decreases their water content and their ability to scatter light at elevated relative humidities [e.g., *Saxena et al.*, 1995; *Carrico et al.*, 2005]. The complexity of the composition of POM and its impact on aerosol optical properties requires the development of simplifying parameterizations that allow for the incorporation of information derived from field measurements into calculations of DCF and visibility [*Kanakidou et al.*, 2004].

[3] We report here an analysis of data from INDOEX, ACE Asia, and ICARTT which has resulted in the development of a parameterization that quantitatively describes the relationship between POM mass fraction and $f_{\sigma sp}(RH)$ for accumulation mode sulfate-POM mixtures. The resulting parameterization specific to POM-sulfate aerosol may be used in combination with $f_{\sigma sp}(RH)$ values assigned to other chemical components for input into RTMs, air quality models, or for the assessment of values of $f_{\sigma sp}(RH)$ currently used in these models. Hence, the parameterization may be used on global or regional scales for any externally mixed aerosol that contains an accumulation mode sulfate-POM mixture.

2. Measurements

[4] During INDOEX, ACE Asia, and ICARTT, simultaneous measurements were made of aerosol chemical composition and $f_{\sigma sp}(RH)$ on one or more platforms. Table 1 gives experimental details. In all cases, nephelometers were used for the determination of $f_{\sigma sp}(RH)$. Values of $f_{\sigma sp}(RH)$ were determined by either scanning over a given RH range (~35 to 85% RH) or by operating two nephelometers in parallel with one at a low RH and one at a high RH (nominally <40% and ~85%). To develop a parameterization to describe the $f_{\sigma sp}(RH)$ behavior of accumulation

[1]Pacific Marine Environmental Laboratory, NOAA, Seattle, Washington, USA.
[2]Aeronomy Laboratory, NOAA, Boulder, Colorado, USA.
[3]Department of Oceanography, University of Hawaii at Manoa, Honolulu, Hawaii, USA.
[4]Aerodyne Research, Inc., Billerica, Massachusetts, USA.
[5]Civil and Environmental Engineering, University of Illinois, Urbana, Illinois, USA.
[6]Climate Monitoring and Diagnostics Laboratory, NOAA, Boulder, Colorado, USA.
[7]School of Earth, Atmospheric, and Environmental Science, University of Manchester, Manchester, UK.
[8]Department of Atmospheric Science, Colorado State University, Fort Collins, Colorado, USA.

0094-8276/05/2005GL024322$05.00

Table 1. Methods for the Measurement of $f_{\sigma sp}(RH)$, $SO_4^=$, and POM Used During INDOEX, ACE Asia, and ICARTT

Experiment	$f_{\sigma sp}(RH)$	$SO_4^=$ and POM	References
INDOEX/KCO[a]	Scanning RH TSI neph.[b]	Impactor[c]	*Chowdhury et al.* [2001]; *Clarke et al.* [2002]
ACE Asia RHB[d]	Scanning RH TSI neph.	Impactor[e]	*Carrico et al.* [2003]; *Quinn et al.* [2004]
ACE Asia Gosan	Scanning RH TSI neph.	AMS[f]	*Topping et al.* [2004]; *Doherty et al.* [2005]
ACE Asia NSF/NCAR C-130	2 RH points RR neph.[g]	Impactor[c]	*Huebert et al.* [2004]; *Doherty et al.* [2005]
ICARTT RHB	Scanning RH TSI neph.	AMS[h]	*Carrico et al.* [2003]
ICARTT CP[i]	Scanning RH TSI neph.	AMS[j]	*Allan et al.* [2005]

[a]KCO, Kaashidhoo Climate Observatory, Maldives.
[b]TSI Nephelometer.
[c]POM = μg C m^3 × 1.4.
[d]RHB, NOAA R/V *Ronald H. Brown*.
[e]POM = μg C m^3 × 1.6.
[f]AMS, Aerosol Mass Spectrometer. Collection efficiency (CE) determined from comparison with impactor measurements.
[g]Radiance Research nephelometer.
[h]CE determined from comparison with number size distribution, impactors, and Particle-into-Liquid Sampler (PILS).
[i]CP, Chebogue Point, Nova Scotia.
[j]CE determined from comparison with number size distribution and impactors.

mode sulfate-POM mixtures, it was necessary to minimize confounding influences from dust and sea salt which reside mainly in the coarse supermicrometer diameter aerosol. Hence, we have used only data that were collected when an impactor with a 1 μm 50% aerodynamic cutoff diameter at 55% RH was upstream of the nephelometers. We further limited the analysis to periods when the submicrometer size range contributed more than 50% to light scattering due to sub-10 μm diameter particles.

[5] Values of $f_{\sigma sp}(RH)$ based on two-point RH measurements were calculated from scattering coefficients measured at a lower, reference RH, $\sigma_{sp}(RH_{ref})$, and at a higher RH, $\sigma_{sp}(RH)$, using

$$f\sigma_{sp}\left(RH, RH_{ref}\right) = \frac{\sigma_{sp}(RH)}{\sigma_{sp}\left(RH_{ref}\right)} \quad (1)$$

where scanning RH measurements were available, measured $f_{\sigma sp}(RH)$ were fit based on observed curve structure [*Carrico et al.*, 2003]. We express $f_{\sigma sp}(RH)$ in terms of γ_s as shown in Equation (2) as this allows the parameterization to be applied to a broader range of RH values [e.g., *Doherty et al.*, 2005]. Here, γ_s is based on RH_{ref} = 40% and RH = 85%. The use of this equation assumes that all particles are deliquesced.

$$\gamma_s = \ln\left(f\sigma_{sp}\left(RH, RH_{ref}\right)\right) \Big/ \ln\left(\frac{100 - RH_{ref}}{100 - RH}\right) \quad (2)$$

[6] On some platforms, $SO_4^=$, NH_4^+, NO_3^-, and organic carbon were measured by collecting particles less than 1 μm aerodynamic diameter with an impactor. $SO_4^=$, NH_4^+, and NO_3^- were analyzed by ion chromatography. Non-sea salt (nss) sulfate was calculated from a sea salt Na^+ to $SO_4^=$ mass ratio of 0.252 [*Holland*, 1978]. Organic carbon (μg C m^{-3}) was determined with a thermo-optical method and multiplied by a factor of 1.4 or 1.6 to convert to POM [*Russell*, 2003]. On other platforms, submicrometer diameter nonrefractory (NR) $SO_4^=$, NH_4^+, NO_3^-, and POM were measured with an Aerodyne Aerosol Mass Spectrometer (AMS). Here, NR refers to any species that volatilizes at ~550°C. The AMS data from all experiments were compared to other instruments to correct for collection efficiencies less than unity (Table 1). The AMS also yields information about the degree of oxidation of the POM based on the fraction of the total POM at mass/charge (m/z) 44 or the m44/POM ratio. The peak at m/z 44 occurs in the mass spectra of heavily oxidized organic species such as di- and poly carboxylic acids [*Allan et al.*, 2004].

[7] The relative amount of POM and sulfate in the submicrometer aerosol was parameterized as F_o where

$$F_o = C_O/(C_O + C_S) \quad (3)$$

and C_O and C_S are the measured mass concentrations of POM and $SO_4^=$, respectively. We focus on these two components since they make up the majority of the submicrometer diameter aerosol mass for the condition imposed here of a contribution of >50% of the measured light scattering by submicrometer aerosol.

3. Results and Discussion

[8] Values of γ_s and F_O for INDOEX were based on measurements made at the Kaashidhoo Climate Observatory (KCO). For ACE Asia, measurements made on the C-130 and the NOAA RV *Ronald H. Brown* (RHB) and at Gosan were merged into one data set and normalized so that all platforms had equal weighting. Similarly, values from RHB and Chebogue Point were merged and normalized for the ICARTT data set. Figure 1 shows F_O versus γ_s and the corresponding linear fit for each region. The linear fits yield the following functions in terms of coefficients ±1 standard deviation for the three different regions

$$ACEAsia: \gamma_s = 0.9(\pm 0.01) - 0.7(\pm 0.01)F_O \quad (4)$$

$$ICARTT: \gamma_s = 0.8(\pm 0.01) - 0.5(\pm 0.01)F_O \quad (5)$$

$$INDOEX: \gamma_s = 0.5(\pm 0.10) - 0.3(\pm 0.20)F_O \quad (6)$$

For all three regions, there is a trend of decreasing γ_s with increasing F_o.

[9] Comparisons between $f_{\sigma sp}(RH)$ derived from measurements (TSI scanning RH nephelometer) and Mie light scattering model calculations show agreement for NaCl and $(NH_4)_2SO_4$ within 10% [*Carrico et al.*, 2003; *Kus et al.*, 2004]. Likewise, RHB measurements of $f_{\sigma sp}(RH)$ at high

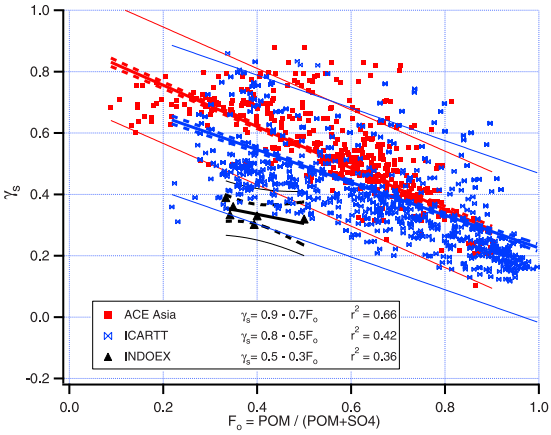

Figure 1. γ_s versus F_o for the three experimental regions. Heavy sold lines represent the linear fit, dashed lines show the 95% confidence level for the fit, and lighter solid lines shows the 95% prediction bands.

RH during ACE Asia from TSI and Radiance Research scanning RH nephelometers demonstrated agreement within 10% for all air mass. Direct comparisons of $f_{\sigma sp}(RH)$ from co-located platforms (C-130, RHB, Gosan) during ACE Asia revealed differences of 10 to 30% [*Doherty et al.*, 2005]. Based on these results, the overall uncertainty when comparing measurements of $f_{\sigma sp}(RH)$ from the three field experiments ranges between 10 and 30%. For $f_{\sigma sp}(85, 40)$, a 10 to 30% change in $f_{\sigma sp}(RH)$ corresponds to a 0.08 to 0.2 change in γ_s. Hence, the linear fits shown in Figure 1 are not significantly different when compared to the overall uncertainty. Merging the ACE Asia and ICARTT data sets and normalizing so that they are weighted equally yields the following single parameterization between γ_s and F_O.

$$\gamma_s = 0.9(\pm 0.003) - 0.6(\pm 0.01)F_O \qquad (7)$$

INDOEX was not included in (7) due to the few data points available and the limited range of F_o over which the measurements were made.

[10] The slope and y-intercept of the fits shown in Figure 1 can be explained, at least in part, by aerosol acidity and $f_{\sigma sp}(RH)$ of the individual aerosol chemical components. Figure 2 shows results from Mie light scattering calculations that describe γ_s as a function of increasing F_O for mixtures of H_2SO_4 – POM, NH_4HSO_4 – POM, and $(NH_4)_2SO_4$ – POM. Values of $f_{\sigma sp}(85, 40)$ of H_2SO_4, NH_4HSO_4, and $(NH_4)_2SO_4$ are based on Mie scattering calculations performed with two assumed particle size distributions (geometric mean particle diameter based on number, D_{gn} = 0.04 μm, geometric standard deviation, σ_{sg} = 1.5 and D_{gn} = 0.2 μm, σ_{sg} = 1.5). These size distributions encompass the range observed during these experiments. Values $f_{\sigma sp}(85, 40)$ of POM equal to 1.1, 1.35, and 1.7 also were assumed. The resulting curves capture most of the observed variability in the $\gamma_s - F_O$ dependence and fall, with a few exceptions, within the ±0.2 measurement uncertainty associated with γ_s.

[11] During ICARTT, RHB encountered continental air masses that left shore and reached the ship with no additional input of urban, industrial, or terrestrial aerosol source material. The shallow stable marine boundary layer minimized mixing from aloft [*Angevine et al.*, 2004] and input of sulfur and POM from the ocean to the marine boundary layer was negligible given the low wind speeds. Under these conditions, the molar ratio of particulate $SO_4^=$ to total sulfur ($SO_4^=$ + gas phase SO_2) can be used as an indicator of the relative age of the sampled aerosol. Relatively young aerosol has a low $SO_4^=/(SO_4^= + SO_2)$ ratio due to insufficient time for conversion of SO_2 to $SO_4^=$ via gas and aqueous phase oxidation processes. As the aerosol ages and more SO_2 is converted to $SO_4^=$, the ratio increases. A comparison of $SO_4^=/(SO_4^= + SO_2)$ to the acidity of the aerosol and the degree of oxidation of the organics suggests that aerosol age determines aerosol chemical composition and, hence, the slope and y-intercept of the $F_O - \gamma_s$ relationship. Using a photochemical age calculated from measured toluene to benzene ratios [*Roberts et al.*, 1984] yields a similar result but goes beyond the analysis presented in this paper.

[12] Figure 3 shows the differences in aerosol chemistry and γ_s as a function of aerosol age during ICARTT on RHB. Younger aerosol was more neutralized having $NH_4^+/(NO_3 + 2SO_4^=)$ molar equivalence ratios near 1 and a higher POM content relative to older aerosol. The POM that was present was less oxidized as indicated by low ratios of m44/POM. This chemical composition led to relatively low values of γ_s. As the aerosol aged, F_O decreased due to increased $SO_4^=$ from the oxidation of SO_2 with no additional significant input of POM. Increased $SO_4^=$ with negligible oceanic sources of NH_3 led to acidification of the aerosol. In addition, the POM became more oxidized. The increased acidity, lower POM content, and higher degree of oxidation within the POM corresponded to higher values of γ_s in accordance with Figure 2. Without knowing the composition of the POM, it is difficult to assess the relative

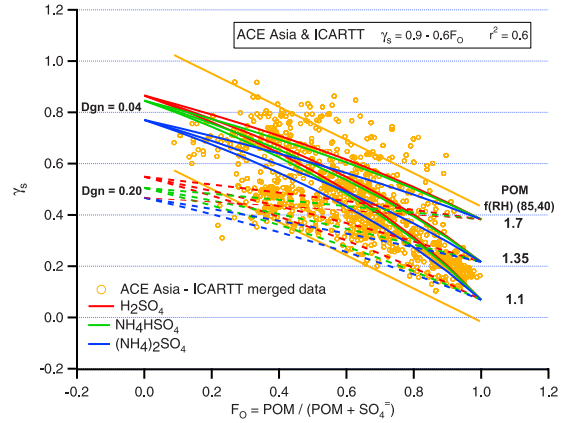

Figure 2. F_O versus γ_s calculated from the assumption of an internally mixed POM – $SO_4^=$ aerosol with 1) a range of POM mass fractions, 2) a sulfate fraction composed of $(NH_4)_2SO_4$, NH_4HSO_4, or H_2SO_4, and 3) POM with $f_{\sigma sp}(RH)$ of 1.1, 1.35, or 1.7. $f_{\sigma sp}(RH)$ (85, 40) for $(NH_4)_2SO_4$, NH_4HSO_4, and H_2SO_4 are based on Mie calculations assuming a size distribution of D_{gn} = 0.04 μm and σ_{sg} = 1.5 (solid lines) and a size distribution of D_{gn} = 0.2 μm and σ_{sg} = 1.5 (dashed lines) Also shown are merged ACE Asia and ICARTT data sets with the 95% prediction bands (solid orange lines).

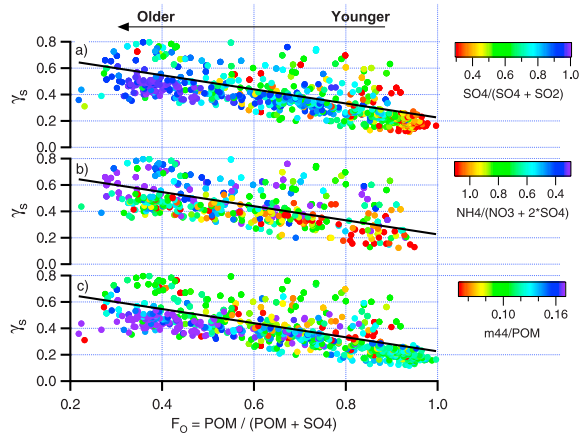

Figure 3. F_O versus γ_s for ICARTT RHB colored as a function of (a) $SO_4^=/(SO_4^= + SO_2)$ molar ratio (relative aerosol age), (b) $NH_4^+/(NO_3^- + 2*SO_4^=)$ equivalence ratio, and (c) m44/POM mass ratio.

importance of aerosol acidity and degree of oxidation of the organics in controlling γ_s.

4. Conclusions

[13] Measurements made downwind of the Indian subcontinent, Asia, and northeastern U.S. all reveal a common trend of decreasing $f_{\sigma sp}(RH)$ with increasing mass fraction of POM. Highest values of $f_{\sigma sp}(RH)$ corresponded to relatively old aerosol that was acidic, had a low POM mass fraction, and a high degree of oxidation of the existing POM. In contrast, lowest values of $f_{\sigma sp}(RH)$ corresponded to younger, more neutralized aerosol that had a higher POM mass fraction containing less oxidized material. Aerosol aging and the resulting chemical processing of the aerosol significantly impact $f_{\sigma sp}(RH)$ of sulfate-POM mixtures.

[14] Based on these data, a relationship between $f_{\sigma sp}(RH)$ and the POM mass fraction has been quantified for accumulation mode sulfate-POM aerosol. This simplified parameterization may be used as input to RTMs to derive values of $f_{\sigma sp}(RH)$ based on CTM estimates of the POM mass fraction. Alternatively, the relationship may be used to assess values of $f_{\sigma sp}(RH)$ currently being employed in RTMs. Similarly, the parameterization may be used in air quality forecast models. Continued simultaneous measurements of $f_{\sigma sp}(RH)$ and aerosol composition at different regions and times of year and the exploration of factors beyond F_O, acidity, and oxidation of the POM will improve the parameterizations presented here.

[15] **Acknowledgments.** This work was supported by the Atmospheric Constituents Program of the NOAA Office of Global Programs, the NOAA Health of the Atmosphere Program, and the New England Air Quality Study. We thank A. R. Ravishankara and anonymous reviewers for helpful comments on the manuscript. This is PMEL paper contribution 2839.

References

Allan, J. D., et al. (2004), Submicron aerosol composition at Trinidad Head, California, during ITCT 2K2: Its relationship with gas phase volatile organic carbon and assessment of instrument performance, *J. Geophys. Res.*, *109*, D23S24, doi:10.1029/2003JD004208.

Allan, J. D., et al. (2005), Detailed in situ measurements of aerosol size, composition, volatility, and hygroscopicity at Chebogue Point, Nova Scotia during ICARTT, paper presented at European Aerosol Conference, Ghent, Belgium, University of Ghent.

Angevine, W. M., et al. (2004), Coastal boundary layer influence on pollutant transport in New England, *J. Appl. Meteorol.*, *43*, 1425–1437.

Carrico, C., P. Kus, M. Rood, P. Quinn, and T. Bates (2003), Mixtures of pollution, dust, seasalt, and volcanic aerosol during ACE-Asia: Aerosol radiative properties as a function of relative humidity, *J. Geophys. Res.*, *108*(D23), 8650, doi:10.1029/2003JD003405.

Carrico, C., et al. (2005), Hygroscopic growth behavior of a carbon-dominated aerosol in Yosemite National Park, *Atmos. Environ.*, *39*, 1393–1404.

Chin, M., et al. (2002), Troposphere aerosol optical thickness from the GOCART model and comparisons with satellite and sun photometer measurements, *J. Atmos. Sci.*, *59*, 461–483.

Chowdhury, Z., L. S. Hughes, L. G. Salmon, and G. R. Cass (2001), Atmospheric particle size and composition measurements to support light extinction calculations over the Indian Ocean, *J. Geophys. Res.*, *106*, 28,597–28,605.

Clarke, A. D., et al. (2002), The INDOEX aerosol: A comparison and summary of chemical, microphysical, and optical properties observed from land, ship, and aircraft, *J. Geophys. Res.*, *107*(D19), 8033, doi:10.1029/2001JD000572.

Doherty, S. J., P. K. Quinn, A. Jefferson, C. M. Carrico, T. L. Anderson, and D. Hegg (2005), A comparison and summary of aerosol optical properties as observed in situ from aircraft, ship, and land during ACE Asia, *J. Geophys. Res.*, *110*, D04201, doi:10.1029/2004JD004964.

Haywood, J. M., V. Ramaswamy, and B. J. Soden (1999), Tropospheric aerosol climate forcing in clear-sky satellite observations over the oceans, *Science*, *283*, 1299–1303.

Holland, H. D. (1978), *The Chemistry of the Atmosphere and Oceans*, 154 pp., John Wiley, Hoboken, N. J.

Huebert, B., T. Bertram, J. Kline, S. Howell, D. Eatough, and B. Blomquist (2004), Measurements of organic and elemental carbon in Asian outflow during ACE-Asia from the NSF/NCAR C-130, *J. Geophys. Res.*, *109*, D19S11, doi:10.1029/2004JD004700.

Kanakidou, M., et al. (2004), Organic aerosol and global climate modelling: A review, *Atmos. Chem. Phys.*, *4*, 5855–6024.

Kus, P., C. M. Carrico, M. J. Rood, and A. Williams (2004), Measured and modeled light scattering values for dry and hydrated laboratory aerosols, *J. Atmos. Oceanic Technol.*, *21*, 981–994.

Quinn, P. K., et al. (2004), Aerosol optical properties measured onboard the *Ronald H. Brown* during ACE-Asia as a function of aerosol chemical composition and source region, *J. Geophys. Res.*, *109*, D19S01, doi:10.1029/2003JD004010.

Roberts, J. M., et al. (1984), Measurements of aromatic hydrocarbon ratios and NO_x concentrations in the rural troposphere: Estimates of air mass photochemical age and NO_x removal rate, *Atmos. Environ.*, *18*, 2421–2432.

Russell, L. (2003), Aerosol organic-mass-to-organic-carbon ratio measurements, *Environ. Sci. Technol.*, *37*, 2983–2987.

Saxena, P., L. J. Hildemann, P. H. McMurry, and J. H. Seinfeld (1995), Organics alter hygroscopic behavior of atmospheric particles, *J. Geophys. Res.*, *100*, 18,755–18,770.

Topping, D., et al. (2004), Aerosol chemical characteristics from sampling conducted on the Island of Jeju, Korea during ACE Asia, *Atmos. Environ.*, *38*, 2111–2123.

J. Allan, School of Earth, Atmospheric, and Environmental Science, University of Manchester, Manchester M60 1QD, UK.

E. Andrews, NOAA CMDL, 325 Broadway, Boulder, CO 80305, USA.

T. S. Bates and D. Coffman, NOAA PMEL, 7600 Sand Point Way NE, Seattle, WA 98115, USA.

T. Baynard, NOAA AL, 325 Broadway, Boulder, CO 80305, USA.

C. M. Carrico, Department of Atmospheric Sciences, Colorado State University, Fort Collins, CO 80523, USA.

A. D. Clarke, Department of Oceanography, University of Hawaii at Manoa, 1000 Pope Rd., Honolulu, HI 96822, USA.

T. B. Onasch and D. Worsnop, Aerodyne Research, Inc., 45 Manning Rd., Billerica, MA 01821, USA.

P. K. Quinn, NOAA PMEL, 7600 Sand Point Way NE, Seattle, WA 98115, USA. (patricia.k.quinn@noaa.gov)

M. J. Rood and W. Wang, Department of Civil and Environmental Engineering, MC-250, University of Illinois, Urbana, IL 61801, USA.